


6th INTERNATIONAL WORKSHOP ON NEW PHOTON-DETECTOR
HARBOUR CENTRE, VANCOUVER (BC) CANADA
19–21 NOVEMBER 2024

nEXO photon detection system and read-out electronics

M.P. Watts  on behalf of the nEXO collaboration

*Wright Laboratory, Department of Physics, Yale University,
272 Whitney Ave, New Haven, CT 06511, U.S.A.*

E-mail: molly.watts@yale.edu

ABSTRACT: nEXO is a next-generation 5-tonne liquid xenon (LXe) time projection chamber that will search for the neutrinoless double beta decay of ^{136}Xe , which is a lepton number violating process that can occur if neutrinos are massive Majorana fermions. The experiment has a projected half-life sensitivity of 1.35×10^{28} years over 10 years of livetime, which sets a design goal of $\lesssim 1\%$ energy resolution (σ_E/E) at the decay Q-value of 2.458 MeV. Achieving this resolution goal requires single photon resolution at the vacuum-ultraviolet scintillation wavelength of LXe of 175 nm while maintaining stringent control of the radiopurity of detector materials. This contribution describes the design optimizations and novel solutions that have led to nEXO's photodetection design, which will instrument approximately 4.5 m² with VUV-sensitive silicon photomultipliers that are read out with cold electronics within the LXe.

KEYWORDS: Cryogenic detectors; Double-beta decay detectors; Noble liquid detectors (scintillation, ionization, double-phase); Photon detectors for UV, visible and IR photons (vacuum) (photomultipliers, HPDs, others)

Contents

1	Introduction	1
2	Conceptual design of nEXO's photon detection system	1
3	Cryogenic read-out electronics	3
4	Conclusions	5

1 Introduction

nEXO is a next-generation single phase liquid xenon (LXe) time projection chamber (TPC) designed to search for neutrinoless double beta decay ($0\nu\beta\beta$) of ^{136}Xe . $0\nu\beta\beta$ is a hypothetical nuclear decay process in which two neutrons decay into two protons, emitting two electrons but no antineutrinos in the final state [1, 2]. This neutrinoless process would differ from the two neutrino double beta decay ($2\nu\beta\beta$) allowed in the Standard Model and observed in several isotopes, in which two antineutrinos are emitted along with two electrons. $0\nu\beta\beta$ can act as a sensitive probe for neutrino properties and physics beyond the Standard Model of particle physics. In particular, if $0\nu\beta\beta$ is observed, it would be the first process that violates lepton number conservation and would indicate that neutrinos are Majorana particles, their own antiparticle. Additionally, measurement of the decay rate may help constrain the absolute neutrino mass scale [3, 4].

nEXO will build on the success of EXO-200, the first experiment to observe $2\nu\beta\beta$ in ^{136}Xe and precisely measure its half-life at $\tau_{1/2} = 2.165 \pm 0.016$ (stat) ± 0.059 (sys) $\times 10^{21}$ yr [5]. The experiment also set a limit on the $0\nu\beta\beta$ process in ^{136}Xe of $T_{1/2}^{0\nu} > 3.5 \times 10^{25}$ yr at a 90% confidence level (CL) with corresponding sensitivity of 5.0×10^{25} yr using an exposure of 234.1 kg·yr [6]. The current most stringent limit on $0\nu\beta\beta$ in ^{136}Xe is set by KamLAND-Zen at $T_{1/2}^{0\nu} > 3.8 \times 10^{26}$ yr (90% CL) [7]. nEXO is designed to probe beyond this parameter space, reaching a sensitivity of 1.35×10^{28} yr at a 90% CL in ten years of data taking. This requires an improved energy resolution of $\sigma_E/E \leq 1\%$ over EXO-200's 1.23% [8]. Due to the near perfect anticorrelation between the scintillation light and ionization signals in LXe [9–11], a combined measurement of the energy deposited in light and charge for each event can achieve improved energy resolution compared to using either channel independently. Since the charge collection efficiency is nearly 100%, while the light detection efficiency for large detectors is typically $\lesssim 10\%$, achieving the required level of sensitivity and energy resolution requires optimizing the photon detector system to maximize the light collection efficiency and minimize readout noise.

2 Conceptual design of nEXO's photon detection system

The characteristic scintillation light of LXe is in the vacuum ultraviolet (VUV) range, with a mean wavelength of 174.8 nm and a full width at half maximum of 10.2 nm [12], and thus requires VUV-sensitive photodetectors. Reaching the design goal of $\sigma_E/E \leq 1\%$, while ensuring that

photodetectors contribute less than 1% to the total background in the region of interest, imposes stringent requirements on both performance and radiopurity [13]. To this end, nEXO will employ VUV-sensitive photomultipliers (SiPMs) that offer lower backgrounds than photomultiplier tubes (PMTs) typically used in LXe detectors for dark matter searches [14, 15] or large area avalanche photodiodes (APDs) previously used in EXO-200 [16], while also providing the performance necessary to meet the experiment’s energy resolution target. Although the APDs used in EXO-200 have higher quantum efficiency [16], the effect of this higher efficiency on the overall detector resolution is outweighed by the higher gain and single photon sensitivity of the SiPMs. SiPMs also provide several engineering advantages, including a high fill factor and lower required bias voltages. For these reasons, SiPMs were chosen as the preferred photodetector technology for nEXO.

The photon detectors used in nEXO must meet stringent performance criteria, including high photon detection efficiency (PDE) in the VUV, low correlated avalanche and dark noise rates, and low intrinsic radioactivity, while operating at cryogenic temperatures in LXe (163 K). These requirements are driven by the experiment’s target energy resolution and background sensitivity goals. In prototype testing, the nEXO collaboration identified two manufacturers of VUV-sensitive devices that meet all performance requirements and enable the experiment to achieve its design energy resolution of $\sigma_E/E \leq 1\%$. These devices are Fondazione Bruno Kessler (FBK) HD3 SiPMs and the VUV4 multi-pixel photon counters (MPPCs) from Hamamatsu Photonics Inc. (HPK) [17]. The final detector design will incorporate 46,000 $1 \times 1 \text{ cm}^2$ SiPMs (figure 1a) with through silicon vias to permit backside attachment and preclude the need for wire bonds on the front, where high electric fields are present. The SiPMs will be grouped in 6 cm^2 read-out channels (figure 1b), with 16 readout channels further assembled onto a “tile module,” which is the basic integrated element of the photon detection system (figure 1c). The tile modules and readout electronics will be further discussed in the next section.

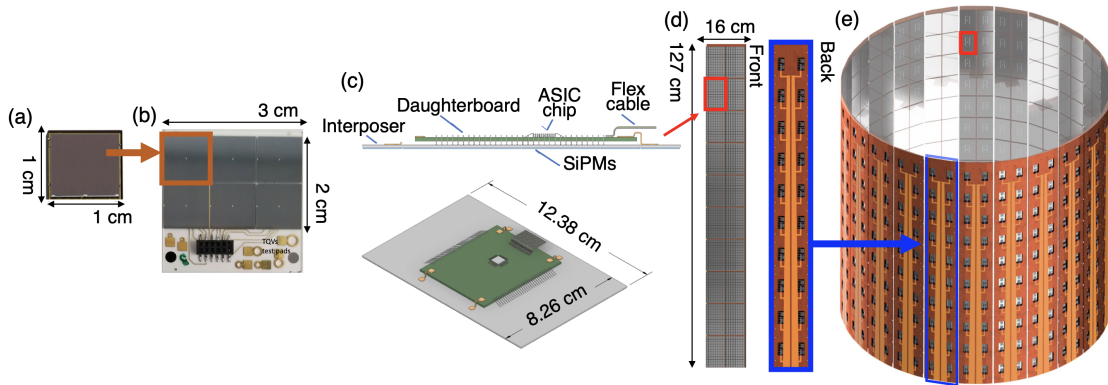


Figure 1. nEXO photon detection system: (a) $1 \times 1 \text{ cm}^2$ SiPM. (b) Prototype fused silica board containing a single $3 \times 2 \text{ cm}^2$ area readout channel comprised of six $1 \times 1 \text{ cm}^2$ SiPMs. The lower section of the prototype board includes test pads and connectors for bias and routing to readout electronics that will not be present in the final design. (c) Side and top views of a tile module, showing SiPMs mounted on an interposer and connected to a daughterboard carrying the readout electronics. (d) Rendering of a single stave, with 20 tile modules shown on the front (left), with a single tile module outlined in red. The back view (right) shows routing to readout daughterboards and signal cables. (e) Full detector configuration, where 24 staves surround the cylindrical barrel of the LXe TPC. A single stave, outlined in blue, shows integrated cabling, and a single tile module placement is outlined in red.

To achieve the required energy resolution of $\leq 1\%$, an overall light detection efficiency of $> 2\%$ is necessary [18]. Previous work on EXO-200 [11] and studies from dual-phase dark matter experiments [19–21], have demonstrated that a light detection efficiency of $\sim 10\%$ can be achieved using a polytetrafluoroethylene (PTFE) reflector around the cylindrical barrel of the detector, with photodetectors positioned only behind transparent anode and cathode planes. However, in nEXO, the use of charge tiles with non-transparent electrodes covering the surface of the anode plane prevents the placement of SiPMs behind the anode.

Chroma simulations of light propagation in the detector indicate that positioning photodetectors only below the cathode (with none above the anode) would result in a photon transport efficiency (PTE) lower than nEXO’s requirements [22]. Here, PTE refers to the fraction of scintillation photons produced in LXe that successfully reach and are absorbed in the active area of a photodetector. Placing photodetectors instead around the cylindrical barrel (outside the field shaping rings) substantially improves the PTE, meeting nEXO requirements. In this configuration, the increased PTE arises primarily from increased sensor area coverage, but is also enhanced by reducing the number of reflections a typical photon will undergo before reaching a sensor, leading to more efficient transport of light to the instrumented area. Studies comparing configurations with photodetectors placed both around the cylindrical barrel and beneath a transparent cathode showed only modest improvements in light collection and possible background rejection relative to the barrel only design. As a result, the additional engineering complexity of instrumenting the cathode was deemed unwarranted.

In the final baseline design for nEXO, tile modules are mounted onto 24 SiPM staves, forming a configuration in which photodetectors encircle the barrel of the detector (figure 1d,e). The full photon detection system provides 4.6 m^2 of photosensitive surface area, with 7,680 readout channels. In this geometry, the field-shaping rings are not enclosed by an optical barrier, creating an optically open field cage that allows scintillation light from both the fiducial volume and surrounding liquid xenon to reach the photosensors without obstruction. This configuration enables detection of light from the “skin” region, i.e., the volume of LXe between the field shaping rings and the SiPMs. Ionization charge is not collected in this region since the electric field does not drift charge to the anode plane outside the field rings. Background events with at least some energy deposition in the skin typically exhibit suppressed ionization but measurable scintillation light, and can be identified by their anomalously low charge-to-light (C/L) ratios. Thus, an effective rejection based on a C/L threshold cut is possible [23], providing a reduction in background compared to the estimates in [24]. Ongoing simulation work analyzing the spatial distribution of detected photons to identify multisite or signal topology from the light patterns projects that this can be further reduced.

3 Cryogenic read-out electronics

Scintillation signals in the nEXO detector will be read out at cryogenic temperatures in LXe (163 K), necessitating low radioactivity front end (FE) electronics integrated within each tile module that operate reliably under these conditions. SiPMs will be mounted to an interposer consisting of a low-radioactivity substrate that provides mechanical support and routing of power and signals to each device. Stringent radioactivity requirements place constraints on the technology and substrate material that can be used, ruling out conventional printed circuit board (PCB) materials, as well as specialized substrates such as Kapton and Cirlex. To meet these requirements, nEXO has explored using 0.6 mm thick fused silica substrates that are similar to the technology developed for the charge readout tiles at

the anode [25]. Fused silica meets the strict radiopurity requirements of nEXO and provides excellent electrical isolation and high-frequency performance. An alternative design utilizing silicon as the interposer substrate material is also being explored as part of ongoing studies [26].

Small-scale prototype fused silica tiles have been produced (figure 1b), and successful operation of single 3×2 SiPM channels mounted on these prototype boards has been demonstrated at Brookhaven National Laboratory. These devices have been shown to both exceed the signal-to-noise ratio and coincidence timing resolution between two subarrays required for nEXO’s sensitivity. Measurements of the prototype’s coincidence timing resolution yield < 20 ns, sufficient for effective rejection of time correlated Bi-Po decay chain backgrounds and for the identification of delayed-coincidence signatures in ^{136}Cs to enable detection of CNO solar neutrinos [27].

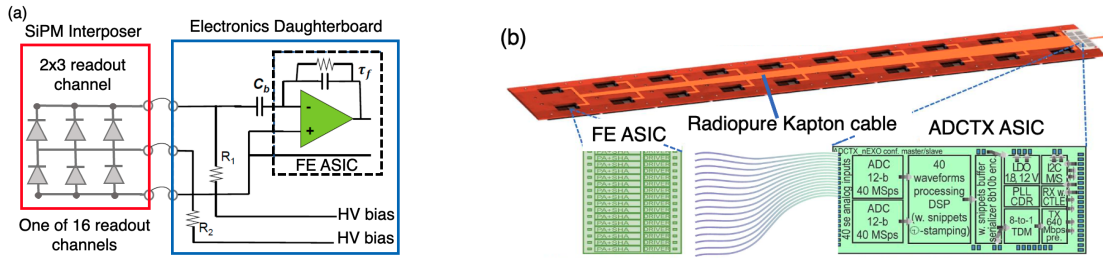


Figure 2. (a) Schematic diagram of readout components. SiPM interposer, showing one of 16 readout channel subarrays outlined in red, connected to a FE ASIC on the daughterboard, outlined in blue. (b) Schematic of stave highlighting one of the 20 tile modules equipped with FE ASIC, handling 16 readout channels. Signals are transmitted via radiopure Kapton cable to an ADCTX ASIC at the top of the stave, which processes signals from all 20 tile modules.

Individual tile modules will process photon signals from 16 of these readout channels, which will be amplified and shaped by an analog front-end application-specific integrated circuit (FE ASIC) located on the daughterboard of the tile module. The daughterboard will also distribute bias voltages to the readout electronics and high voltage bias to the SiPMs. Each readout channel in nEXO will integrate six $1 \times 1 \text{ cm}^2$ SiPMs, in a $3 \times 2 \text{ cm}^2$ array. This array size is chosen as it provides the largest channel size that satisfies noise specifications, since capacitance grows with channel size, while maintaining sufficient granularity to resolve the light distribution of events at the edge of the detector’s fiducial volume. To further reduce capacitance, the readout channels utilize a configuration in which 3 SiPMs are connected in parallel and 2 such parallel connections are connected in series (3P2S) (figure 2a).

Tile modules will be mounted on staves, with each stave containing 20 tile modules. Signals from the analog FE ASICs propagate along a radiopure Kapton cable to an ASIC containing analog-to-digital converters (ADCs), located at the top of each stave, to digitize signals for further processing (figure 2b). The stave-orientated design, containing digital electronics only at the top of the stave, reduces cable mass, which minimizes background contributions. The placement of the ADC ASICs at the top of the stave also minimizes any risk associated with nucleate boiling of LXe in regions of the detector where high electric fields are present [28]. Digitized signals are then multiplexed and transmitted to the data acquisition system located outside the cryogenic system.

4 Conclusions

nEXO has developed a mature conceptual design for a full photon detection system. The experiment will employ 46,000 SiPMs as the photodetector technology, chosen for their low intrinsic radioactivity and ability to achieve nEXO's energy resolution goal of $< 1\%$. Measurement and characterization efforts have identified prototype devices from two vendors that not only meet but exceed performance requirements. SiPMs will be positioned around the cylindrical barrel of the detector in an optically open field cage, providing a design that accommodates opaque charge tiles at the anode plane, while optimizing photon transport efficiency and maintaining radiopurity. This novel configuration enables detailed light patterns to be reconstructed across the pixellated SiPM array, enabling background discrimination for events with incomplete charge collection near the detector edges.

In parallel, nEXO's readout electronics are designed to operate at cryogenic LXe temperatures, while meeting strict radiopurity requirements. The system integrates fused silica interposers, low-capacitance SiPM readout configurations, and a stove-orientated design with Kapton cables to minimize backgrounds and optimize signal processing. The design choices of the detector's architecture and electronic readout system ensure achieving the design goal of $\lesssim 1\%$ energy resolution (σ_E/E) to reach the projected sensitivity to $0\nu\beta\beta$ at the 10^{28} yr scale.

Acknowledgments

This material is based upon work supported by the National Science Foundation Graduate Research Fellowship under Grant No. DGE-2139841. nEXO is supported by the Office of Nuclear Physics within DOE's Office of Science, and NSF in the United States; NSERC, CFI, FRQNT, NRC, and the McDonald Institute (CFREF) in Canada; IBS in Korea; and CAS and NSFC in China. This work was supported in part by Laboratory Directed Research and Development (LDRD) programs at Brookhaven National Laboratory (BNL), Lawrence Livermore National Laboratory (LLNL), Oak Ridge National Laboratory (ORNL), Pacific Northwest National Laboratory (PNNL), and SLAC National Accelerator Laboratory.

References

- [1] W.H. Furry, *On transition probabilities in double beta-disintegration*, *Phys. Rev.* **56** (1939) 1184.
- [2] W. Rodejohann, *Neutrino-less Double Beta Decay and Particle Physics*, *Int. J. Mod. Phys. E* **20** (2011) 1833 [[arXiv:1106.1334](#)].
- [3] I.I.I.F.T. Avignone, S.R. Elliott and J. Engel, *Double Beta Decay, Majorana Neutrinos, and Neutrino Mass*, *Rev. Mod. Phys.* **80** (2008) 481 [[arXiv:0708.1033](#)].
- [4] J. Engel and J. Menéndez, *Status and Future of Nuclear Matrix Elements for Neutrinoless Double-Beta Decay: A Review*, *Rept. Prog. Phys.* **80** (2017) 046301 [[arXiv:1610.06548](#)].
- [5] EXO-200 collaboration, *Observation of Two-Neutrino Double-Beta Decay in ^{136}Xe with EXO-200*, *Phys. Rev. Lett.* **107** (2011) 212501 [[arXiv:1108.4193](#)].
- [6] EXO-200 collaboration, *Measurements of the ion fraction and mobility of α - and β -decay products in liquid xenon using the EXO-200 detector*, *Phys. Rev. C* **92** (2015) 045504 [[arXiv:1506.00317](#)].
- [7] KAMLAND-ZEN collaboration, *Search for Majorana Neutrinos with the Complete KamLAND-Zen Dataset*, [arXiv:2406.11438](#).

- [8] EXO-200 collaboration, *Search for Neutrinoless Double- β Decay with the Complete EXO-200 Dataset*, *Phys. Rev. Lett.* **123** (2019) 161802 [[arXiv:1906.02723](#)].
- [9] EXO-200 collaboration, *Correlated fluctuations between luminescence and ionization in liquid xenon*, *Phys. Rev. B* **68** (2003) 054201 [[hep-ex/0303008](#)].
- [10] M. Szydagis et al., *NEST: A Comprehensive Model for Scintillation Yield in Liquid Xenon*, *2011 JINST* **6** P10002 [[arXiv:1106.1613](#)].
- [11] EXO-200 collaboration, *Measurement of the scintillation and ionization response of liquid xenon at MeV energies in the EXO-200 experiment*, *Phys. Rev. C* **101** (2020) 065501 [[arXiv:1908.04128](#)].
- [12] K. Fujii et al., *High-accuracy measurement of the emission spectrum of liquid xenon in the vacuum ultraviolet region*, *Nucl. Instrum. Meth. A* **795** (2015) 293.
- [13] nEXO collaboration, *nEXO: neutrinoless double beta decay search beyond 10^{28} year half-life sensitivity*, *J. Phys. G* **49** (2022) 015104 [[arXiv:2106.16243](#)].
- [14] L. Baudis et al., *Characterisation of Silicon Photomultipliers for Liquid Xenon Detectors*, *2018 JINST* **13** P10022 [[arXiv:1808.06827](#)].
- [15] XENON collaboration, *Lowering the radioactivity of the photomultiplier tubes for the XENONIT dark matter experiment*, *Eur. Phys. J. C* **75** (2015) 546 [[arXiv:1503.07698](#)].
- [16] R. Neilson et al., *Characterization of large area APDs for the EXO-200 detector*, *Nucl. Instrum. Meth. A* **608** (2009) 68 [[arXiv:0906.2499](#)].
- [17] nEXO collaboration, *Performance of novel VUV-sensitive Silicon Photo-Multipliers for nEXO*, *Eur. Phys. J. C* **82** (2022) 1125 [[arXiv:2209.07765](#)].
- [18] nEXO collaboration, *nEXO Pre-Conceptual Design Report*, [[arXiv:1805.11142](#)].
- [19] B.J. Mount et al., *LUX-ZEPLIN (LZ) Technical Design Report*, [[arXiv:1703.09144](#)].
- [20] XENON collaboration, *The XENONnT dark matter experiment*, *Eur. Phys. J. C* **84** (2024) 784 [[arXiv:2402.10446](#)].
- [21] PANDA X collaboration, *Dark Matter Search Results from 1.54 Tonne-Year Exposure of PandaX-4T*, *Phys. Rev. Lett.* **134** (2025) 011805 [[arXiv:2408.00664](#)].
- [22] A. Jamil, *Rare Event Searches in Liquid Xenon with EXO-200, nEXO and Beyond*, Ph.D. Thesis, Yale University (2022).
- [23] nEXO collaboration, *Event reconstruction in a liquid xenon Time Projection Chamber with an optically-open field cage*, *Nucl. Instrum. Meth. A* **1000** (2021) 165239 [[arXiv:2009.10231](#)].
- [24] nEXO collaboration, *Sensitivity and Discovery Potential of nEXO to Neutrinoless Double Beta Decay*, *Phys. Rev. C* **97** (2018) 065503 [[arXiv:1710.05075](#)].
- [25] nEXO collaboration, *Characterization of an Ionization Readout Tile for nEXO*, *2018 JINST* **13** P01006 [[arXiv:1710.05109](#)].
- [26] J.-F. Pratte et al., *3D Photon-To-Digital Converter for Radiation Instrumentation: Motivation and Future Works*, *Sensors* **21** (2021) 598.
- [27] S. Haselschwardt, B. Lenardo, P. Pirinen and J. Suhonen, *Solar neutrino detection in liquid xenon detectors via charged-current scattering to excited states*, *Phys. Rev. D* **102** (2020) 072009 [[arXiv:2009.00535](#)].
- [28] P.A. Breur et al., *Measurement of the onset of nucleate boiling in liquid xenon*, *2021 JINST* **16** T02004 [[arXiv:2007.11124](#)].